

University of Groningen

The role of immunoediting in lymphomas of immune-privileged sites

Booman, Marije

IMPORTANT NOTE: You are advised to consult the publisher's version (publisher's PDF) if you wish to cite from it. Please check the document version below.

Document Version

Publisher's PDF, also known as Version of record

Publication date:

2008

[Link to publication in University of Groningen/UMCG research database](#)

Citation for published version (APA):

Booman, M. (2008). *The role of immunoediting in lymphomas of immune-privileged sites*. s.n.

Copyright

Other than for strictly personal use, it is not permitted to download or to forward/distribute the text or part of it without the consent of the author(s) and/or copyright holder(s), unless the work is under an open content license (like Creative Commons).

The publication may also be distributed here under the terms of Article 25fa of the Dutch Copyright Act, indicated by the "Taverne" license. More information can be found on the University of Groningen website: <https://www.rug.nl/library/open-access/self-archiving-pure/taverne-amendment>.

Take-down policy

If you believe that this document breaches copyright please contact us providing details, and we will remove access to the work immediately and investigate your claim.

Downloaded from the University of Groningen/UMCG research database (Pure): <http://www.rug.nl/research/portal>. For technical reasons the number of authors shown on this cover page is limited to 10 maximum.

Chapter 5

Genomic alterations and gene expression in primary diffuse large B-cell lymphomas of immune-privileged sites: the importance of apoptosis and immunomodulatory pathways

Marije Booman, Karoly Szuhai, Andreas Rosenwald, Elena
Hartmann, Hanneke C Kluin-Nelemans, Daphne de Jong, Ed
Schuuring and Philip M Kluin

A shorter version of this chapter has been submitted to Journal of Pathology

Abstract

Primary diffuse large B-cell lymphomas of different immune-privileged sites (IP-DLBCL) share many clinical and biological features, such as a relatively poor prognosis, preferential dissemination to other immune-privileged sites and deletion of the HLA region, which suggests that IP-DLBCL represents a separate entity.

To further investigate the nature of IP-DLBCL, we investigated site-specific genomic aberrations in 16 testicular, 9 central nervous system (CNS) and 15 nodal DLBCL using array-CGH. We also determined minimal common regions of gain and loss. Using robust algorithms, the array-CGH data were combined with gene expression data to explore pathways deregulated by chromosomal aberrations.

Loss of 6p21.32–p25.3, including the HLA genes, was associated with both types of IP-DLBCL, whereas gain of 2p16.1–p25.3 was associated with nodal DLBCL. Gain of 12q15–q21.1 and 12q24.32–q24.33 was associated with CNS DLBCL and gain of 19q13.12–q13.43 with testicular DLBCL. Analysis of candidate genes in site-specific regions and minimal common regions revealed two major groups of genes: one involved in the immune response, including regulation of HLA expression and another involved in apoptosis, including the p53 pathway. Many of these genes were also involved in homozygous deletions or high level gains.

The presence of both shared and site-specific aberrations in CNS and testicular DLBCL underlines the concept of IP-DLBCL but also indicates that IP-DLBCL of the CNS and testis do not form a single entity. The observed aberrations emphasize the importance of the deregulation of anti-tumor immune response and apoptosis pathways.

Introduction

Primary diffuse large B-cell lymphoma (DLBCL) represents a heterogeneous group of lymphomas, which is reflected by clinical features, (histo)pathology, genomic aberrations and gene expression profiles (reviewed in ref. 1). Two major subtypes of DLBCL are recognized, associated with differences in prognosis: the activated B cell-like (ABC) and germinal centre B cell-like (GCB).² These subtypes can be distinguished by gene expression profile^{3,4} or immunohistochemistry⁵ and are associated with specific genomic aberrations.^{6–8}

Primary testicular DLBCL and primary DLBCL of the central nervous system (CNS) are part of the immune-privileged site-associated DLBCL (IP-DLBCL) and share characteristics that separate them from nodal (non-IP) DLBCL. Besides having a different clinical behavior^{9,10} and being predominantly of the ABC subtype,^{11–13} we demonstrated a prominent loss of HLA class I and II (gene) expression, often caused by small interstitial deletions of chromosome 6p21.3.^{14,15} This is associated with a downregulation of many immune-associated genes and a diminished infiltration of T cells.¹⁵ Deletions at 6p21.3 account for loss of HLA expression in approximately 50% of IP-DLBCL and in much less non-IP DLBCL cases,¹⁶ indicating the presence of alternative mechanisms.¹⁵

The shared characteristics between testicular and CNS DLBCL suggest that these IP-DLBCL subtypes belong to the same homogeneous entity, that is separate from nodal non-IP DLBCL. So far no studies have compared genomic aberrations and gene expression between these groups of DLBCL. To that end, we explored genomic aberrations in testicular, CNS and nodal DLBCL. We combined these data with gene expression data obtained from the same cases and used robust algorithms to identify deregulated candidate genes in the aberrant chromosomal regions.

Materials and methods

Tissue sample collection and selection

Fifty frozen samples from 19 primary testicular, 12 primary CNS and 19 primary nodal DLBCL were collected from tissue banks at the University Medical Center Groningen, Leiden University Medical Center, Josefine Nefkens Institute, Rotterdam; Netherlands Cancer Institute, Amsterdam, The Netherlands and University of Würzburg, Germany. Only samples from patients with Ann Arbor stage I or II were selected; the minimum number of tumor cells was 50%. All 50 cases were used for gene expression analysis. Due to insufficient quality of

array-comparative genomic hybridization (CGH) results we performed array-CGH analysis on 40 of the 50 cases: 16 testicular, 9 CNS and 15 nodal DLBCL. This study was approved by the institutional board of the UMCG and carried out in accordance with the modified Declaration of Helsinki.

Gene expression microarray hybridization

Total RNA was isolated using TRIzol reagent (Invitrogen, Carlsbad, CA, USA) according to the manufacturers' instructions. The samples were processed and hybridized on Affymetrix HG U133 plus 2.0 oligonucleotide arrays (Affymetrix, Santa Clara, CA, USA) following the protocol for eukaryotic samples in the Expression Analysis Technical Manual (http://www.affymetrix.com/support/technical/manual/expression_manual.affx). The average probe array signals were scaled to a target signal of 500 using the GeneChip operating software GCOS (Affymetrix). Probesets with a signal below 50 were discarded, leaving a final dataset of 29381 probesets.

ABC/GCB analysis

Array expression data of 25 genes were used to determine the ABC/GCB subtype of the lymphomas with the linear predictor score (LPS) method.⁴ Nineteen testicular and 5 of the nodal DLBCL cases were previously characterized for ABC/GCB subtype on another microarray platform.¹¹ Of these, only 1 testicular DLBCL was reclassified from GCB to ABC.

Global gene expression analysis

Global gene expression comparison was performed using SAM analysis¹⁷ in the R package Siggenes (<http://bioconductor.org/packages/2.1/bioc/html/siggenes.html>). Before comparing global gene expression between testicular, CNS and nodal DLBCL, we excluded 2 datasets from the analysis: one ABC/GCB-specific set to avoid bias due to the skewed ABC/GCB proportions in IP-DLBCL, and one set of genes that are differently expressed between normal CNS and normal testis to minimize the effect of 'contaminating' normal tissue. The ABC/GCB-specific dataset was determined by SAM analysis of the 19 nodal DLBCL (9 ABC and 10 GCB) using a FDR cutoff of 0.05, and consisted of 360 genes (451 probesets). The genes that are differently expressed between normal testis and CNS tissue were identified using the GNF Human HG133A/GNF1H Tissue Atlas dataset.¹⁸ For each gene, the average expression values in normal testis and normal CNS tissue were determined. After testing several fold difference cutoffs (data not shown), 645 genes (807 probesets) that showed an 8-fold or higher difference in expression between normal testis and normal CNS tissue were removed from the dataset for global gene expression analysis. The final global gene expression comparison was performed on a dataset of 28131 probesets, using an FDR cutoff of 0.01.

Array-CGH analysis

Genomic DNA was isolated using high salt after overnight SDS/proteinase K digestion and hybridized on an in house printed CGH array containing ~3700 large genomic insert clones (provided by Dr. N. Carter, Wellcome Trust Sanger Institute, UK), as previously described.¹⁹ Log₂ ratio values were analyzed using R packages DNACopy²⁰ and aCGH/MergeLevels²¹ to determine regions and levels of gain and loss. Hemi- and homozygous loss were defined as one and two levels lower than normal respectively, gain as one or two levels higher than normal, and high level gain as three or more levels higher than normal.²¹ Chromosomes X and Y were excluded from further analysis, as well as heterochromatic regions, centromeres, ribosomal gene clusters and regions with known segmental duplications (grey areas in FIGURE 1). Minimal common regions (MCR) were defined as the smallest regions of overlap that were smaller than 20 Mb and present in at least 4 cases, of which at least 3 showed a limited aberration smaller than a whole chromosome or chromosomal arm. Overrepresentation of aberrations in different localizations was assessed using the Fisher Exact test.

Combining expression and array-CGH data

ACE-it version 2.1²² was used to find genes for which expression levels correlate with genomic gain or loss. In short, for each lymphoma a status of gain, normal or loss was assigned (without distinction between hemi- and homozygous loss, or between single copy and high level gain) to each base pair position based on the array-CGH data. This status was mapped to the Affymetrix probesets. The correlation of expression levels with genomic loss/gain was analyzed for each probe set by comparing expression in cases with loss/gain with expression in cases without aberrations using a one-sided non-parametric Wilcoxon test with Benjamini and Hochberg multiplicity correction. Genes for which expression correlated with gain or loss were annotated through the Entrez ID using DAVID (<http://david.abcc.ncifcrf.gov/home.jsp>), focusing on candidate genes with a known function in oncogenesis, normal B cells or B-cell neoplasms for which loss or gain would be functionally relevant for the tumor cells.

Results

Differences in gene expression and genomic aberrations between testicular, CNS and nodal DLBCL

Using the LPS method, most testicular (17 of 19) and CNS (7 of 9) DLBCL were determined as ABC subtype, whereas in nodal DLBCL the balance was more equal: 9 of 19 ABC and 10 of 19 GCB subtype. After removal of genes that were significantly associated with the ABC/GCB subtype or differently expressed between normal testis and CNS, global gene expression analysis of the 3 DLBCL groups revealed significant differences: 1036 genes were differentially expressed between testicular and CNS DLBCL, 2847 between testicular and nodal DLBCL, and 665 between CNS and nodal DLBCL. As expected,¹⁵ the expression of HLA class I and class II genes was significantly lower in both testicular and CNS DLBCL, however Gene Set Enrichment Analysis²³ did not disclose any other biologically/functionally interesting patterns (data not shown).

To investigate specific genomic aberrations in testicular and CNS DLBCL we performed array-CGH analysis (FIGURE 1). The average number of aberrations per case was 9.9 in testicular, 8.9 in CNS and 9.4 in nodal DLBCL. Homozygous losses were found in 16 regions, high level gains in 6 regions. The most common aberrations, present in at least 30% of CNS, testicular or nodal DLBCL cases, are shown in TABLE 1. TABLE 2 summarizes the 5 regions showing significant overrepresentation in one or more localizations.

To identify candidate genes in these 5 localization-specific regions we combined gene expression analysis with array-CGH analysis using ACE-it. Significant genes whose expression levels correlated with genomic loss or gain were screened for a known function in oncogenesis, normal B cells or B-cell neoplasms (TABLE 2; full list of all significant genes in SUPPLEMENTARY TABLE S1). We described alterations of HLA and other genes at 6p21.32–p25.3 previously;¹⁵ this region is not further discussed here. Gain of 2p16.1–p25.3 was associated exclusively with nodal DLBCL. This region contained 32 significantly altered genes including candidates SUPT7L and anti-apoptotic BIRC6 and BRE. Gain of both 12q15–q21.1 and 12q24.23–q24.33 was associated with CNS DLBCL. The 12q15–q21.1 region contained 8 significantly altered genes including candidates MDM2 and YEATS4 that are tightly associated with p53. The 12q24.32–q24.33 region contained 10 significantly altered genes but none with a relevant function. Gain of 19q13.12–q13.43 was associated with testicular DLBCL. This region is very gene dense and contained 83 significantly altered genes, including 5 candidates LILRA3, SPIB, BCL2L12, PAK4 and PPP5C.

Analysis of gene expression in minimal common regions

We extended the combined array-CGH/expression analysis to the minimal common regions (MCR). In all 40 DLBCL combined, 30 regions met our criteria for an MCR: 15 with

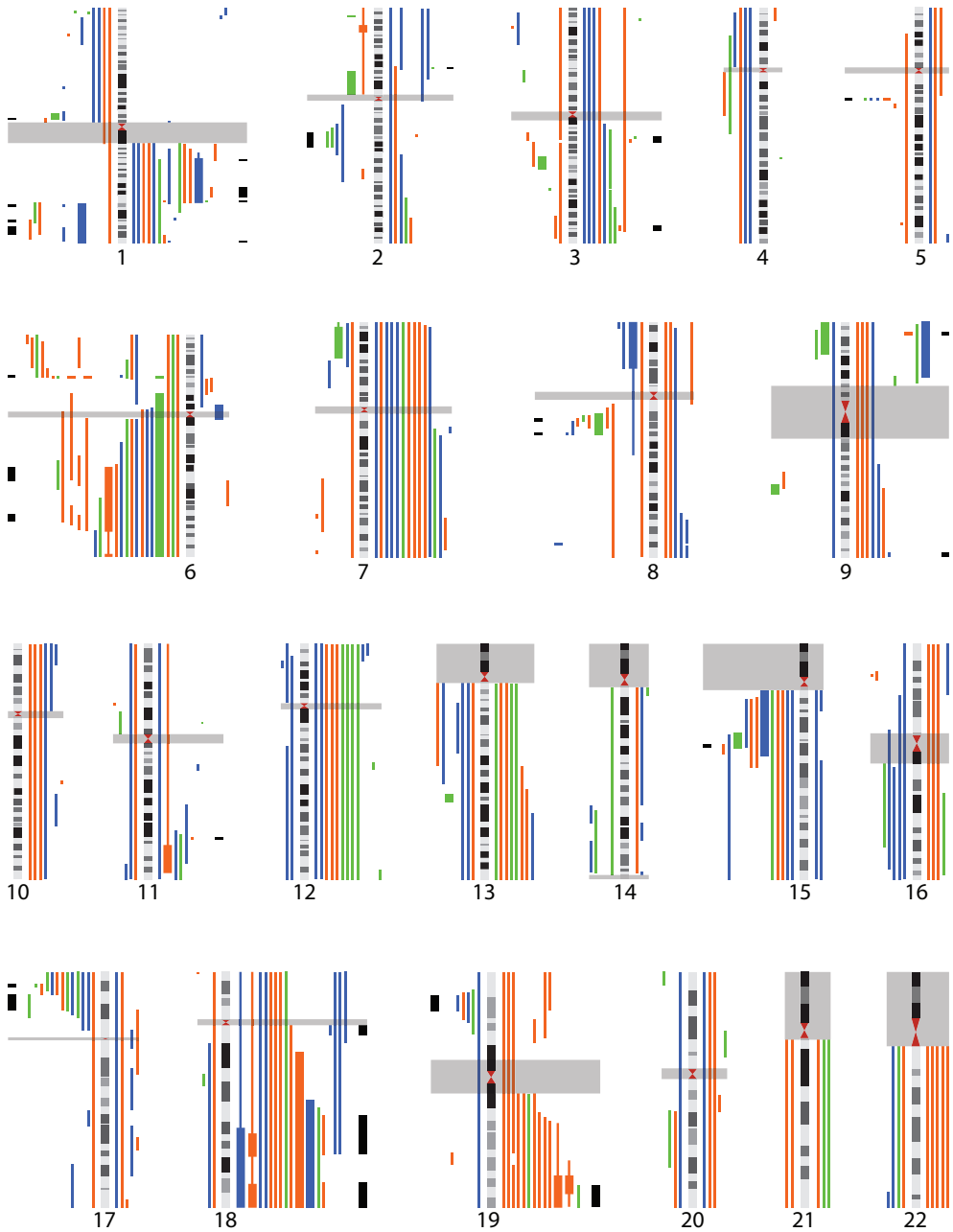


Figure 1. Genomic aberrations found in CNS, testicular and nodal DLBCL using array-CGH analysis

Losses (left) and gains (right) in testicular (orange), CNS (green) or nodal DLBCL (blue). Homozygous deletions and high level gains are indicated by thick colored bars. MCRs are indicated by thick black bars on the left- and rightmost side for each chromosome. Grayed out areas were excluded.

Table 1. Most common genomic aberrations in CNS, testicular and nodal DLBCL

	All cases (n = 40)	CNS DLBCL (n = 9)	Testicular DLBCL (n = 16)	Nodal DLBCL (n = 15)
Loss				
6p21.32–p25.2	18 (45%)	5 (56%)	11 (69%)	2 (13%)
6q	20 (50%)	5 (56%)	10 (63%)	5 (33%)
15q12–q21.1	12 (30%)	2 (22%)	5 (31%)	5 (33%)
17p12–p13.3	13 (33%)	5 (56%)	4 (25%)	4 (27%)
Gain				
1q21.3–q32.1	15 (38%)	3 (33%)	7 (44%)	5 (33%)
7/7q	14 (35%)	2 (22%)	6 (38%)	6 (40%)
12	9 (23%)	4 (44%)	3 (19%)	2 (13%)
18p	11 (28%)	1 (11%)	4 (25%)	6 (40%)
18q	15 (38%)	2 (22%)	7 (44%)	6 (40%)
19q13.12–q13.43	13 (33%)	2 (22%)	11 (69%)	0 (0%)

Aberrations in 30% or more of CNS, testicular or nodal DLBCL are listed. For each site the number of cases (and percentage) in which an aberration occurs is indicated.

Table 2. Site-specific aberrations and candidate genes

	Location (Mb)	All cases (n = 40)	CNS (n = 9)	Testicular (n = 16)	Nodal (n = 15)	Significant higher frequency in*:	Candidate genes
Loss							
6p21.32–p25.2	1–34,919	18 (45%)	5 (56%)	11 (69%)	2 (13%)	IP-DLBCL	†
Gain							
2p16.1–p25.3	1–60,560	4 (10%)	0 (0%)	0 (0%)	4 (27%)	nodal DLBCL	SUPT7L, BIRC6, BRE
12q15–q21.1	66,251–71,743	10 (25%)	5 (56%)	3 (19%)	2 (13%)	CNS DLBCL	MDM2, YEATS4
12q24.32–q24.33	125,033–132,450	10 (25%)	5 (56%)	3 (19%)	2 (13%)	CNS DLBCL	—
19q13.12–q13.43	37,665–63,812	13 (33%)	2 (22%)	11 (69%)	0 (0%)	testicular DLBCL	LILRA3, SPIB, BCL2L12, PAK4, PPP5C

Aberrations that differ in frequency between CNS, testicular and nodal DLBCL, and the candidate genes located therein. The number of cases (and percentage) in which an aberration occurs is indicated for each site.

* $p < 0.05$ using Fisher Exact test

† Gene expression in this region has been studied previously.¹⁵

Mb: megabase.

gain and 15 with loss (black bars in FIGURE 1). TABLE 3 lists each region together with the number of genes significant in ACE-it analysis and the candidate genes of interest (Full lists of significantly altered genes in SUPPLEMENTARY TABLE S1; site-specific frequency data in SUPPLEMENTARY TABLE S2).

Discussion

Primary IP-DLBCL share many features including a frequent dissemination to other immune-privileged sites.^{9,24,25} This suggests that these lymphomas share important biological features such as a similar expression of adhesion molecules, homing receptors or chemokines and their receptors.^{26,27} We previously demonstrated that IP-DLBCL share a prominent downregulation of HLA class I and class II proteins, caused by small interstitial deletions at chromosome 6p21.3 in approximately 50% of cases.^{14,15} These observations led us to investigate whether IP-DLBCL share more functional and genomic features that separate them from nodal non-IP DLBCL.

Our approach focused on genomic gains and losses defined by array-CGH and the concomitant alterations in gene expression. This approach has the strong advantage that the gene expression alterations related to the microenvironment are filtered out. Five chromosomal regions showed significant differences in copy number between testicular, CNS and nodal DLBCL (TABLE 2). This included loss of 6p21.32–p25.2, which has been found previously in more than 50% of IP-DLBCL^{14,15} and in mediastinal large B-cell lymphomas (PMLBCL)²⁸ and causes loss of HLA class I and II expression.

Aberrations that were more frequently found in CNS DLBCL than in other cases were gain of 12q15–q21.1 and 12q24.32–q24.33. We identified 2 candidate genes in the first region: YEATS4, a repressor of the p53 pathway,²⁹ and MDM2, which is an inhibitor of p53 via ubiquitin-dependent proteasomal degradation.³⁰ High expression of MDM2 was recently reported to be associated with gain of chromosome 12 and poor prognosis in mantle cell lymphoma³¹ and was also suggested to be a candidate in PMLBCL.²⁸ Weber et al.³² described a similar gain of 12q13–14 and 12q24 in CNS DLBCL but they did not study other DLBCL, nor did they correlate their results with gene expression. They also identified a frequent high level gain of 18q21, however in our series gain of this region, with BCL2 and MALT1 being candidate genes, was not specific for CNS DLBCL (TABLE 3 and SUPPLEMENTARY TABLE S2). According to the literature gain of 18q21 is often associated with ABC-type DLBCL rather than with a specific site of DLBCL.^{7,30} High level gain of 9p23–p24 was also described in CNS DLBCL.³² We observed this gain in 1 CNS, 4 testicular and 2 nodal DLBCL (SUPPLEMENTARY TABLE S2); again indicating that many of the previously reported aberrations are not site-specific.

Table 3. MCR regions and candidate genes

Cytoband	Location (Mb)	Size (Mb)	All cases (n = 40)	Annotated known genes			Candidate genes
				Total	In array dataset	Correlating with gain/loss	
Loss							
1p12–p13.2	114,446–118,301	3.48	7 (18%)	31	17	4 (24%)	—
1q32.2–q32.3	203,602–208,089	4.49	5 (13%)	28	19	4 (21%)	—
1q42.11–q42.13	220,131–225,195	5.06	5 (13%)	51	39	11 (28%)	PARP1
1q42.2–q43	227,397–237,217	9.82	5 (13%)	45	33	9 (27%)	EGLN1
2q14.3–q22.2	127,254–143,617	16.36	4 (10%)	63	35	18 (51%)	ERCC3, MAP3K2
5q13.1–q13.2	67,677–71,660	3.98	5 (13%)	30	18	0 (0%)	—
6p21.32–p22.1	29,496–33,468	3.97	15 (38%)	154	111	*	*
6q16.3–q21	100,953–112,430	11.48	18 (45%)	52	36	24 (67%)	REV3L, ATG5
6q23.3–q24.2	137,302–144,432	7.13	18 (45%)	26	18	16 (89%)	HIVEP2, PERP, PLAGL1, TNFAIP3
8q12.1–q12.2	58,379–61,851	3.47	8 (20%)	9	6	5 (83%)	—
8q13.1–q13.3	67,344–72,600	5.26	6 (15%)	23	15	3 (20%)	—
15q15.3–q21.1	41,852–45,135	3.28	12 (30%)	27	19	10 (53%)	PDIA3
17p13.2	3,399–6,065	2.67	12 (30%)	57	40	24 (60%)	PFN1, ITGAE
17p12–p13.1	7,438–12,92	5.48	8 (20%)	61	38	13 (34%)	TP53, MAP2K4
19p13.2–p13.3	5,893–12,007	6.11	5 (13%)	156	104	32 (31%)	SMARCA4
Gain							
1q23.2–q23.3	156,697–160,910	4.21	12 (30%)	69	51	25 (49%)	CD48, FRET, PEA15
1q31.1–q31.2	185,925–198,884	12.96	12 (30%)	51	34	15 (44%)	—
1q32.1	199,641–202,973	3.33	13 (33%)	50	32	9 (28%)	—
1q44	241,691–245,523	3.83	8 (20%)	54	14	4 (29%)	—
2p15–p16.1	60,754–62,654	1.90	6 (15%)	12	12	4 (33%)	—
3q13.12–q13.13	107,671–111,576	3.90	8 (20%)	14	7	3 (43%)	CD47
3q13.13–q13.2	110,272–114,747	4.48	8 (20%)	27	21	5 (24%)	—
3q26.33–q28	183,353–189,732	6.38	9 (23%)	63	42	19 (45%)	PARL
9p24.1	5,121–8,399	3.28	7 (18%)	20	16	4 (25%)	PDCD1LG2
9q34.2–q34.3	133,750–138,429	4.68	7 (18%)	86	61	1 (2%)	—
11q22.3–q23.1	108,393–112,571	4.18	6 (15%)	27	20	4 (20%)	—
18q11.1–q11.2	16,100–21,431	5.33	13 (33%)	22	20	3 (15%)	—
18q21.1–q21.33	45,188–59,059	13.87	15 (38%)	50	34	19 (56%)	POLI, BCL2, MALT1
18q22.3–q23	66,930–76,117	9.19	13 (33%)	25	23	12 (52%)	—
19q13.41–q13.43	56,504–63,812	7.31	13 (33%)	217	136	42 (31%)	LILRA3

Regions containing homozygous losses or high level gains are indicated in bold.

* Gene expression in this region has been studied previously.¹⁵

Mb: megabase.

An aberration that was more frequently found in testicular DLBCL than in other cases was gain of 19q13.12–q13.43. One array-CGH study⁷ reported on this gain in approximately 50% of nodal ABC-type DLBCL, which could not be confirmed in our nodal cases and was rarely identified in other series of B-cell lymphomas analyzed by array-CGH (ref. 28 and Progenetix database <http://www.progenetix.de>). Eighty-three genes in this region were higher expressed in cases with gain, of which 5 were interesting candidate genes. LILRA3 is part of the leukocyte immunoglobulin-like receptor (LILR) gene family that contains both activating and inhibitory LILR genes (reviewed in ref. 33). LILRA3 exists in a soluble form. High expression by the lymphoma cells might therefore act as an antagonist (by competing for ligand) for activating LILRs on tumor-infiltrating lymphocytes. Three other candidate genes have a role in inhibition of apoptosis: BCL2L12, a recently discovered member of the BCL2 gene family,³⁴ PAK4, which functions in TNF α -induced pro-survival pathways³⁵ and PPP5C, which inhibits p53-induced apoptosis as well as the MAP2K4/JNK pathway.³⁶ The fifth potential target gene is SPIB, which is deregulated by chromosomal translocation t(14;19) in the ABC-type DLBCL cell line OCI-Ly3³⁷ and is a direct target of the transcription factor BOB1 in normal B cells.³⁸ Interestingly, in two of our testicular DLBCL SPIB is located at the transition point of normal gain to high level gain, suggesting that deregulated expression is triggered by this rearrangement.

An aberration that was more frequently found in nodal DLBCL than in other cases was gain of 2p16.1–p25.3. The candidates BIRC6 and BRE are anti-apoptotic genes^{39,40} and SUPT7L (ARTC1) has been reported to be a ligand for anti-tumor regulatory T cells in melanoma,⁴¹ overexpression leading to suppression of the local anti-tumor immune response. Two well known targets of 2p amplification in DLBCL, REL and BCL11A,⁴² were not marked as potential targets in our series since REL expression did not correlate with gain, and BCL11A was located outside both the nodal-specific region and the MCR of 2p15–p16.1.

Apart from these site-specific chromosomal regions we identified MCRs and the candidate genes therein. Interestingly, a large proportion of the candidate genes from both analyses is involved in either apoptosis or regulation of the immune response/HLA (TABLE 4).

Regarding apoptosis, interesting candidates showing loss are PARP1 (at 1q42.12) that is fundamentally involved in DNA damage control and apoptosis in B-cell lymphomas,⁴³ the pro-apoptotic tumor suppressor gene MAP2K4⁴⁴ and TP53 (both located in the MCR at 17p12–p13.1). Loss of TP53 in DLBCL is associated with an aggressive clinical behavior.⁴⁵ Loss of 6q23.3–q24.2 (including homozygous deletion in 2 IP-DLBCL) was associated with down-regulation of PERP, a direct effector of apoptosis downstream of TP53. Using SNP analysis PERP was recently described as a candidate tumor suppressor gene for follicular lymphoma.⁴⁶ Interestingly, in our series 27 of 40 cases (8 of 9 CNS, 12 of 16 testicular, 7 of 15 nodal) showed genomic aberrations affecting the p53 pathway (loss of TP53 or PERP or gain of MDM2), suggesting that this pathway is an important target for deregulation in DLBCL.

Table 4. Functionally interesting genes whose expression correlate with gain or loss

Apoptosis	Immune response and HLA regulation	Proliferation and migration
ATG5		PFN1
BCL2	CD47	PLAGL1
BCL2L12	CD48	
BIRC6	ITGAE	DNA repair
BRE	LILRA3	ERCC3
EGLN1	PDCD1LG2	
MALT1	PDIA3	NFκB pathway
MAP2K4	SMARCA4	TNFAIP3
MAP3K2	SUPT7L	
MDM2		
PAK4	B-cell signaling	
PARL	FREB	
PARP1	SPIB	
PEA15		
PERP	Somatic hypermutation	
PPP5C	POLI	
TP53	REV3L	
YEATS4		

Genes involved in homozygous loss or high level gain are indicated in bold type. The genes are derived from Tables 2 and 3.

Deletion of 6p21.32 is the major mechanism by which HLA class II expression is lost in IP-DLBCL.^{14,15} However, low expression without deletion is also found in IP-DLBCL and nodal DLBCL.^{15,16} Loss of SMARCA4 and disruption of the interferon gamma pathway might be an alternative mechanism for loss of HLA expression. SMARCA4 is located in the MCR at 19p13.2 and is essential for the interferon gamma-induced chromatin remodeling of class II transactivator (CIITA), which is the major regulator of HLA class II expression.⁴⁷ Another factor in the interferon gamma pathway, IFNGR1, is located in the MCR at 6q23.3–q24, but its expression did not correlate with genomic loss in our data. We also observed loss (including homozygous deletion in two cases) of PDIA3 at 15q15.3, which interacts with calnexin/calreticulin and tapasin in the MHC class I peptide loading complex.⁴⁸

Apart from downregulation of HLA, other mechanisms are deployed to escape the anti-tumor immune response. Gain (including high level gain) of 9p24.1 was associated with higher expression of PDCD1LG2, which is a ligand of the ‘programmed cell death receptor’ on T cells; binding to this receptor inhibits T-cell activation.⁴⁹ A consistently increased expression of this gene, often caused by gain of 9p24, has been described in PMLBCL.⁵⁰ Also gain of LILRA3 at 19q13, discussed earlier, belongs in this category.

In conclusion, genomic differences between IP-DLBCL and nodal DLBCL exist, the most prominent being the hemi- and homozygous deletions of 6p21.32 in IP-DLBCL. The presence of different aberrations in CNS and testicular DLBCL implies that these DLBCL do not form a homogeneous entity. Using robust algorithms that selected for alterations within tumor cells

we found a striking selection for genes involved in apoptosis, including the p53 pathway, as well as for genes that can modulate the anti-tumor immune response.

Acknowledgements

The authors would like to thank Marja van der Burg for hybridizing the CGH arrays. EH is supported by the Interdisciplinary Center for Clinical Research (IZKF).

References

- De Paepe P, De Wolf-Peeters C. Diffuse large B-cell lymphoma: a heterogeneous group of non-Hodgkin lymphomas comprising several distinct clinicopathological entities. *Leukemia* 2007;21: 37–43.
- Alizadeh AA, Eisen MB, Davis RE, et al. Distinct types of diffuse large B-cell lymphoma identified by gene expression profiling. *Nature* 2000;403: 503–11.
- Rosenwald A, Wright G, Chan WC, et al. The use of molecular profiling to predict survival after chemotherapy for diffuse large-B-cell lymphoma. *N Engl J Med* 2002;346: 1937–47.
- Wright G, Tan B, Rosenwald A, Hurt EH, Wiestner A, Staudt LM. A gene expression-based method to diagnose clinically distinct subgroups of diffuse large B cell lymphoma. *Proc Natl Acad Sci U S A* 2003;100: 9991–6.
- Hans CP, Weisenburger DD, Greiner TC, et al. Confirmation of the molecular classification of diffuse large B-cell lymphoma by immunohistochemistry using a tissue microarray. *Blood* 2004;103: 275–82.
- Bea S, Zettl A, Wright G, et al. Diffuse large B-cell lymphoma subgroups have distinct genetic profiles that influence tumor biology and improve gene-expression-based survival prediction. *Blood* 2005;106: 3183–90.
- Tagawa H, Suguro M, Tsuzuki S, et al. Comparison of genome profiles for identification of distinct subgroups of diffuse large B-cell lymphoma. *Blood* 2005;106: 1770–7.
- Iqbal J, Sanger WG, Horsman DE, et al. BCL2 translocation defines a unique tumor subset within the germinal center B-cell-like diffuse large B-cell lymphoma. *Am J Pathol* 2004;165: 159–66.
- Zucca E, Conconi A, Mughal TI, et al. Patterns of outcome and prognostic factors in primary large-cell lymphoma of the testis in a survey by the International Extranodal Lymphoma Study Group. *J Clin Oncol* 2003;21: 20–7.
- Schlegel U, Schmidt-Wolf IGH, Deckert M. Primary CNS lymphoma: clinical presentation, pathological classification, molecular pathogenesis and treatment. *J Neurol Sci* 2000;181: 1–12.
- Booman M, Douwes J, Glas AM, de Jong D, Schuurin E, Kluin PM. Primary testicular diffuse large B cell lymphomas have activated B cell-like subtype characteristics. *J Pathol* 2006;210: 163–71.
- Camilleri-Broet S, Criniere E, Broet P, et al. A uniform activated B-cell-like immunophenotype might explain the poor prognosis of primary central nervous system lymphomas: Analysis of 83 cases. *Blood* 2006;107: 190–6.
- Lin CH, Kuo KT, Chuang SS, et al. Comparison of the expression and prognostic significance of differentiation markers between diffuse large B-cell lymphoma of central nervous system origin and peripheral nodal origin. *Clin Cancer Res* 2006;12: 1152–6.
- Riemersma SA, Jordanova ES, Schop RF, et al. Extensive genetic alterations of the HLA region, including homozygous deletions of HLA class II genes in B-cell lymphomas arising in immune-privileged sites. *Blood* 2000;96: 3569–77.
- Booman M, Douwes J, Glas AM, et al. Mechanisms and effects of loss of HLA class II expression in immune privileged site-associated B-cell lymphoma. *Clin Cancer Res* 2006;12: 2698–705.
- Rimsza LM, Roberts RA, Campo E, et al. Loss of major histocompatibility class II expression in non-immune privileged site diffuse large B cell lymphoma is highly coordinated and not due to chromosomal deletions. *Blood* 2006;107: 1101–7.
- Tusher VG, Tibshirani R, Chu G. Significance analysis of microarrays applied to the ionizing radiation response. *Proc Natl Acad Sci U S A* 2001;98: 5116–21.
- Su AI, Wiltshire T, Batalov S, et al. A gene atlas of the mouse and human protein-encoding transcriptomes. *Proc Natl Acad Sci U S A* 2004;101: 6062–7.
- Knijnenburg J, Szuhai K, Giltay J, et al. Insights from genomic microarrays into structural chromosome rearrangements. *Am J Med Genet A* 2005;132: 36–40.
- Venkatraman ES, Olshen AB. A faster circular binary segmentation algorithm for the analysis of array CGH data. *Bioinformatics* 2007;23: 657–63.
- Willenbrock H, Fridlyand J. A comparison study: applying segmentation to array CGH data for downstream analyses. *Bioinformatics* 2005;21: 4084–91.
- van Wieringen WN, Belien JAM, Vosse SJ, Achame EM, Ylstra B. ACE-it: a tool for genome-wide integration of gene dosage and RNA expression data. *Bioinformatics* 2006;22: 1919–20.

23. Subramanian A, Tamayo P, Mootha VK, et al. Gene set enrichment analysis: A knowledge-based approach for interpreting genome-wide expression profiles. *Proc Natl Acad Sci U S A* 2005; 102: 15545–50.
24. Fonseca R, Habermann TM, Colgan JP, et al. Testicular lymphoma is associated with a high incidence of extra-nodal recurrence. *Cancer* 2000; 88: 154–61.
25. Rajappa SJ, Uppin SG, Digumarti R. Testicular relapse of primary central nervous system lymphoma. *Leuk Lymphoma* 2007; 48: 1023–5.
26. Smith JR, Brazier RM, Paoletti S, Lipp M, Uguccioni M, Rosenbaum JT. Expression of B-cell-attracting chemokine 1 (CXCL13) by malignant lymphocytes and vascular endothelium in primary central nervous system lymphoma. *Blood* 2003; 101: 815–21.
27. Rubenstein J, Fridlyand J, Shen A, et al. Gene expression and angiotropism in primary CNS lymphoma. *Blood* 2006; 107: 3716–23.
28. Wessendorf S, Barth TFE, Viardot A, et al. Further delineation of chromosomal consensus regions in primary mediastinal B-cell lymphomas: an analysis of 37 tumor samples using high-resolution genomic profiling (array-CGH). *Leukemia* 2007; DOI: 10.1038/sj.leu.2404919.
29. Park JH, Roeder RG. GAS41 is required for repression of the p53 tumor suppressor pathway during normal cellular proliferation. *Mol Cell Biol* 2006; 26: 4006–16.
30. Rao PH, Houldsworth J, Dyomina K, et al. Chromosomal and gene amplification in diffuse large B-cell lymphoma. *Blood* 1998; 92: 234–40.
31. Hartmann E, Fernandez V, Stoecklein H, Hernandez L, Campo E, Rosenwald A. Increased MDM2 expression is associated with inferior survival in mantle-cell lymphoma, but not related to the MDM2 SNP309. *Haematologica* 2007; 92: 574–5.
32. Weber T, Weber RG, Kaulich K, et al. Characteristic chromosomal imbalances in primary central nervous system lymphomas of the diffuse large B-cell type. *Brain Pathol* 2000; 10: 73–84.
33. Brown D, Trowsdale J, Allen R. The LILR family: modulators of innate and adaptive immune pathways in health and disease. *Tissue Antigens* 2004; 64: 215–25.
34. Stegh AH, Kim H, Bachoo RM, et al. Bcl2L12 inhibits post-mitochondrial apoptosis signaling in glioblastoma. *Genes Dev* 2007; 21: 98–111.
35. Li X, Minden A. PAK4 functions in tumor necrosis factor (TNF) alpha-induced survival pathways by facilitating TRADD binding to the TNF receptor. *J Biol Chem* 2005; 280: 41192–200.
36. Zhou G, Golden T, Aragon IV, Honkanen RE. Ser/Thr protein phosphatase 5 inactivates hypoxia-induced activation of an apoptosis signal-regulating kinase 1/MKK-4/JNK signaling cascade. *J Biol Chem* 2004; 279: 46595–605.
37. Lenz G, Nagel I, Siebert R, et al. Aberrant immunoglobulin class switch recombination and switch translocations in activated B cell-like diffuse large B cell lymphoma. *J Exp Med* 2007; 204: 633–43.
38. Bartholdy B, Du Roure C, Bordon A, Emslie D, Corcoran LM, Matthias P. The Ets factor Spi-B is a direct critical target of the coactivator OBF-1. *Proc Natl Acad Sci U S A* 2006; 103: 11665–70.
39. Hao Y, Sekine K, Kawabata A, et al. Apollon ubiquitinates SMAC and caspase-9, and has an essential cytoprotection function. *Nat Cell Biol* 2004; 6: 849–60.
40. Li Q, Ching AK, Chan BC, et al. A death receptor-associated anti-apoptotic protein, BRE, inhibits mitochondrial apoptotic pathway. *J Biol Chem* 2004; 279: 52106–16.
41. Wang HY, Peng G, Guo Z, Shevach EM, Wang RF. Recognition of a new ARTC1 peptide ligand uniquely expressed in tumor cells by antigen-specific CD4+ regulatory T cells. *J Immunol* 2005; 174: 2661–70.
42. Fukuhara N, Tagawa H, Kameoka Y, et al. Characterization of target genes at the 2p15-16 amplicon in diffuse large B-cell lymphoma. *Cancer Sci* 2006; 97: 499–504.
43. Dukers DF, Oudejans JJ, Vos W, ten Berge RL, Meijer CJ. Apoptosis in B-cell lymphomas and reactive lymphoid tissues always involves activation of caspase 3 as determined by a new in situ detection method. *J Pathol* 2002; 196: 307–15.
44. Teng DHF, Perry III WL, Hogan JK, et al. Human mitogen-activated protein kinase kinase 4 as a candidate tumor suppressor. *Cancer Res* 1997; 57: 4177–82.
45. Bea S, Colomo L, Lopez-Guillermo A, et al. Clinicopathologic significance and prognostic value of chromosomal imbalances in diffuse large B-cell lymphomas. *J Clin Oncol* 2004; 22: 3498–506.

46. Ross CW, Ouillette PD, Saddler CM, Shedden KA, Malek SN. Comprehensive analysis of copy number and allele status identifies multiple chromosome defects underlying follicular lymphoma pathogenesis. *Clin Cancer Res* 2007; 13: 4777–85.
47. Ni Z, Karaskov E, Yu T, et al. Apical role for BRG1 in cytokine-induced promoter assembly. *Proc Natl Acad Sci U S A* 2005; 102: 14611–6.
48. Zhang Y, Williams DB. Assembly of MHC class I molecules within the endoplasmic reticulum. *Immunol Res* 2006; 35: 151–62.
49. Saunders PA, Hendrycks VR, Lidinsky WA, Woods ML. PD-L2:PD-1 involvement in T cell proliferation, cytokine production, and integrin-mediated adhesion. *Eur J Immunol* 2005; 35: 3561–9.
50. Rosenwald A, Wright G, Leroy K, et al. Molecular diagnosis of primary mediastinal B cell lymphoma identifies a clinically favorable subgroup of diffuse large B cell lymphoma related to Hodgkin lymphoma. *J Exp Med* 2003; 198: 851–62.